Journal of Alloys and Compounds 591 (2014) 263–267

Contents lists available at ScienceDirect

Journal of Alloys and Compounds

journal homepage: www.elsevier.com/locate/jalcom

Bulk-like behavior in the temperature driven martensitic transformation of Cu–Zn–Al thin films with 2H structure

N. Haberkorn [a,*], A.M. Condó [a,b], C. Espinoza [b], S. Jaureguizahar [a,b], J. Guimpel [a,b], F.C. Lovey [a,b]

[a] Centro Atómico Bariloche, CNEA, Bustillo 9500, S.C. de Bariloche, Argentina
[b] Instituto Balseiro, Bustillo 9500, S.C. de Bariloche, Argentina

ARTICLE INFO

Article history:
Received 11 September 2013
Received in revised form 11 December 2013
Accepted 12 December 2013
Available online 25 December 2013

Keywords:
Metals and alloys
Microstructure
Phase transitions
Shape memory
Thin films

ABSTRACT

This paper reports on the possibility to obtain Cu–Zn–Al films with 2H martensitic structure by fixing the valence electron concentration per atom (e/a) ≈1.53. Films with thickness of ≈5 μm with micrometric grains show martensitic transformation temperature and hysteresis values close to the ones found in bulk samples. This result is different to the one found in Cu–Zn–Al thin films with 18R martensitic structure and similar microstructure, in which the hysteresis presents an increment (≈10 times) compared to bulk samples. This difference can be associated to the intrinsic nature of the 2H transformation which requires more undercooling to produce the nucleation of the martensitic phase. The driving force for the burst-type martensitic transformation decreases the influence of the microstructure in the transformation.

1. Introduction

Shape memory alloys (SMA) are materials with two outstanding properties: shape memory and pseudo elasticity, which arise due a martensitic transformation [1]. The martensitic transformation can be induced and reversed by cooling and heating (giving rise to the shape memory effect), or by applying and withdrawing mechanical stress (giving rise to the pseudo elastic effect). These properties appear as particularly advantageous in the development of micro-electromechanical systems (MEMS) [2,3]. The technological applications are based on the possibility of modifying properties such as shape, stiffness or natural frequency in response to temperature or stress, or to an external magnetic field [4–6]. The development of micro and nanometric systems based in SMA requires an understanding of the response of these properties when the dimensionality is reduced. Many studies and reports which discuss the influence of the microstructure and the dimensionality have been performed in Ni–Ti [7–9], and more recently, the performance of other SMA has been evaluated [4,5,10,11]. For example, studies in Cu–Al–Ni nanopillars [10,11] show that the super elastic behavior is higher than that reported in Ni–Ti nanopillars [12] of similar diameter. This fact indicates that depending on SMA different functionalities can be obtained. In this way, Cu-based SMA have some particular characteristics such as the stabilization of different structures which show a wide range of martensitic start transformation temperatures (M_s) and different hysteresis widths [13,14]. At high temperature the β phase structure in Cu–Zn–Al alloys adopts a bcc structure. During the cooling process and depending on the composition, a cubic B2 or a cubic $L2_1$ structure could be adopted. The lattice parameter of the cubic $L2_1$ superstructure cell doubles the lattice parameter of the corresponding bcc structure. The transformation austenite (β phase → 18R martensite ($1.46 < e/a < 1.52$) in bulk is associated with a small temperature hysteresis ≈5 K, whereas the hysteresis for the β → 2H martensite transformation ($1.52 < e/a < 1.532$) is considerably higher ≈20–30 K [15,16]. In the latter case, the β →2H transformation is a consequence of nucleation difficulties which result from an abrupt or burst-type martensitic transformation.

The resulting properties in SMA thin films are usually affected by the microstructure. A high density of grain boundaries and the finite size of grains could induce transformation strains and interfaces which hinder the transformation, and change both the thermal stability of the martensite and its transformation path. For instance, the properties of Ni-Ti thin films were shown to strongly depend on metallurgical factors and preparation conditions [17–19]. Grain boundaries as well as surface degradation [20] play an important role in Ni–Ti films sub micrometric samples. Recently, we have been able to tune the M_s in Cu–Zn–Al films with β → 18R martensitic transformation [21]. However, the films presented a transformation hysteresis of 35–50 K, which is larger than the typical value found in bulk samples (≈5 K). This difference could be associated with the fact that grain boundaries can act as obstacles that hinder the transformation by impeding the lateral

* Corresponding author. Tel.: +54 0294 444 5147; fax: +54 0294 444 5299.
E-mail address: nhaberk@cab.cnea.gov.ar (N. Haberkorn).

0925-8388/$ - see front matter © 2013 Elsevier B.V. All rights reserved.
http://dx.doi.org/10.1016/j.jallcom.2013.12.109

expansion of thin martensite plates due to the constraints imposed by the presence of adjacent sub micrometric grains [22]. Although low dimensional systems show a good performance related to the mechanical response, their temperature-driven martensitic phase transformation can be affected due to the increasing role of the surface/volume ratio [9,23]. Even though many studies about the influence of the microstructure have been performed in the Ni–Ti system, its influence on the response of other SMA remains unexplored in depth. As the Cu–Zn–Al system presents more than one martensitic structure, it allows to investigate the response of different martensitic structures in samples grown by the same method (similar microstructure). Although several investigations on this ternary system with 2H martensite have been published [14–16], no study has been performed in films with micrometric grain size.

This work reports the presence of β → 2H martensitic transformation in polycrystalline Cu–Zn–Al films with thickness $t \approx 5$ μm. The grain size of the films obtained depends on the chemical concentration of the alloy, with averages between 1 and 4 μm. It has been noticed that the M_s and hysteresis in pure β films are similar to those found in bulk (in contraposition to the β → 18R martensitic transformation). In the same way, the hysteresis is incremented due to the presence of γ-phase precipitates. This confirms that in samples with similar microstructure the type of martensitic structure plays an important role in the features of the resulting transformation.

2. Experimental

Binary precursor films were grown from targets with nominal composition Cu–23.40 at.% Al (film precursor: P1) and Cu–25.44 at.% Al (film precursor: P2) by DC magnetron sputtering on Si (1 0 0) without intentional heating of the substrate, under 10 mTorr of argon, and a power of 50 W. Samples were grown without intentional heating to avoid chemical reactions between the silicon substrate and the aluminum of the precursor film, which complicate the peeling off of the films from the substrates. The pre-vacuum in the sputtering chamber was 1×10^{-6} Torr. The targets (diameter: 38 mm, height: 4 mm) were prepared with pure metals melted in an encapsulated quartz tube under argon atmosphere. During the deposition, the substrate was located above the target at 70 mm. Deposition sputtering rate was estimated from cross section scanning electron microscope images (not shown), showing a growth rate of ~50 nm/min.

After growth, the Cu–Al films were easily peeled off from the substrates and encapsulated in quartz tubes under an argon atmosphere (diameter: 8 mm, length ≈ 50 mm) inside a tantalum envelope, together with a Cu–Zn–Al bulk reference (~1 gr.) for reactive annealing. During the thermal annealing, a vapor atmosphere of Zn is created by the Cu–Zn–Al reference sample. The Cu–Al film absorbs Zn atoms until equilibrium with vapor of Zn is established. Thus, the Cu–Al film copies the Zn chemical concentration of the reference alloy, which in this case the Al/Cu ratio is the same as in the precursor film [21]. The annealing temperature is selected to obtain Zn diffusion and the corresponding β equilibrium phase during the same process. It is worth mentioning that Zn evaporation in Cu–Zn–Al samples in argon atmosphere become important over 973 K, due to a very thin Al_2O_3 protective layer on the surface [24]. These bulk references were prepared considering a valence electron concentration (e/a) = 1.53 to obtain the 2H martensite [15]. The nominal chemical composition of the references were Cu–11.66 at.% Zn–20.67 at.% Al (R1) and Cu–4.51 at.% Zn–24.24 at.% Al (R2) aiming at values of martensitic transformation temperature (M_s) estimated at 175 K and 315 K, respectively. The values of M_s were estimated considering M_s [K] = (301–798 (C_{Zn} + 1.03 C_{Al}))/(0.51(e/a)–0.58)–15 (where C_i is the atomic fraction of the i element, and (15) in the last term is half the hysteresis) [25]. This equation considers the changes of the enthalpy and entropy between the austenite and 2H martensite phases [15,16]. The Al to Cu ratio proportion is the same within the pairs (P1, R1) and (P2, R2). These pairs were heated from room temperature to 1123 K at 5 K/min, annealed during one hour, and finally quenched in iced water. The whole process (opening the furnace, breaking the quartz ampoule and introducing the sample into water) is performed in less than 5 s. The ternary films obtained were called F1 and F2 for the pairs (P1, R1) and (P2, R2), respectively. The annealing temperature of 1123 K was selected to obtain the β phase, according to the stability range in the ternary Cu–Zn–Al phase diagram [26]. The structure of the films was studied by transmission electron microscopy (TEM) with a Philips CM200UT microscope operating at 200 kV. TEM specimens were prepared using standard ion milling techniques in a Gatan PIP system. The films were characterized by X-ray diffraction (XRD) in a Philips PW 1710 diffractometer using Cu Kα radiation, steps of 0.02° and 1 s acquisition time. The martensitic transformation was characterized by electrical transport using conventional four-probe geometry in a vacuum cooling machine with a temperature rate (cool down and warming up) of 1 K/min.

3. Results and discussion

Fig. 1 shows resistance vs. temperature for both films studied and for R1. The parameters of the martensitic transformation are summarized in Table 1. It has been noticed that the $M_s \approx 140$ K in film F1 is slightly lower than in reference R1 ($M_s \approx 150$ K), although the hysteresis of the transformation ($\Delta T \approx 30$ K) is nearly the same. Film F2 shows a value of $M_s \approx 290$ K which is again lower than the experimental value obtained for reference R2 ($M_s \approx 320$ K). This difference in M_s can be attributed to small changes in the chemical concentration of the Cu–Al sputtered film, which directly affect the absolute M_s value, i.e., changes of 0.1 at.% in the Al concentration of the binary film are enough to shift 5–7 K the M_s of the final Cu–Zn–Al film (see equation for M_s estimation in experimental section). In addition, in film F2 the hysteresis is larger ($\Delta T \approx 42$ K) than the one present in reference R2 ($\Delta T \approx 20$ K). This could be related to the presence of nanometric γ-phase precipitates (see TEM results below), since it has been reported that the hysteresis becomes wider with the presence of small precipitates [27]. On the other hand, the reference R2 was annealed at high temperature (1273 K) in order to avoid γ-phase precipitates and the hysteresis was considerably reduced.

Fig. 2a shows an X-ray diffraction pattern of film F1 at room temperature where only peaks corresponding to the β phase are present and indicate that the sample is polycrystalline. The peaks

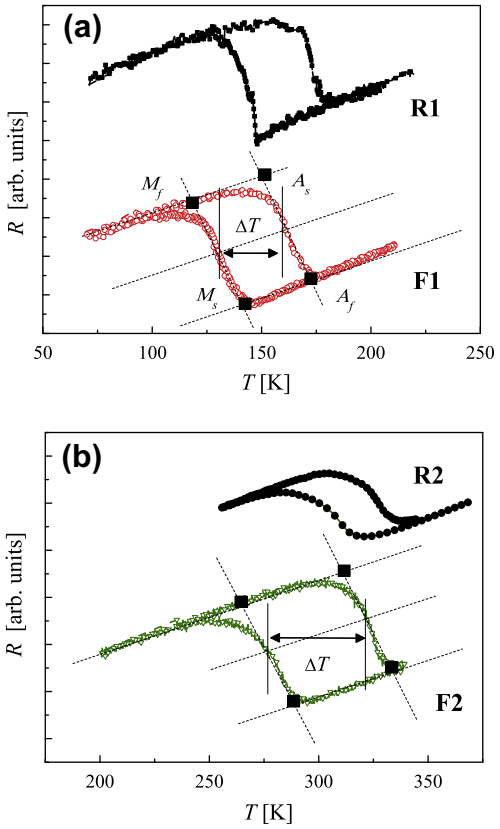

Fig. 1. Resistance vs. temperature in the reference R1 and in the films F1 and F2. The method for defining the parameters of the martensitic transformation was included. The hysteresis is measured as ΔT. On cooling, the transformation temperature is set to start at M_s and to go to completion at M_f. On heating, the retransformation is set to start at the A_s temperature and finish at A_f. The resistance was rescaled for a clearer presentation.

Table 1
Measured transformation temperatures in the reference samples and in the films obtained by reactive annealing. The transformation temperatures are defined as indicated in Fig. 1. A_S: start of the retransformation to austenite, A_F: end of the retransformation to austenite, M_S: start of the martensitic transformation temperature, M_F: end of the martensitic transformation temperature. The hysteresis (ΔT) of the martensitic transformation was also included for each sample.

Sample	M_s (K)	M_f (K)	A_s (K)	A_f (K)	ΔT (K)
Reference R1	150	135	170	180	30
Film F1	140	120	150	170	30
Reference R2[a]	320	295	315	340	20
Film F2	290	265	305	330	42

[a] Ref. [2] was annealed at 1273 K in order to avoid γ-phase precipitates.

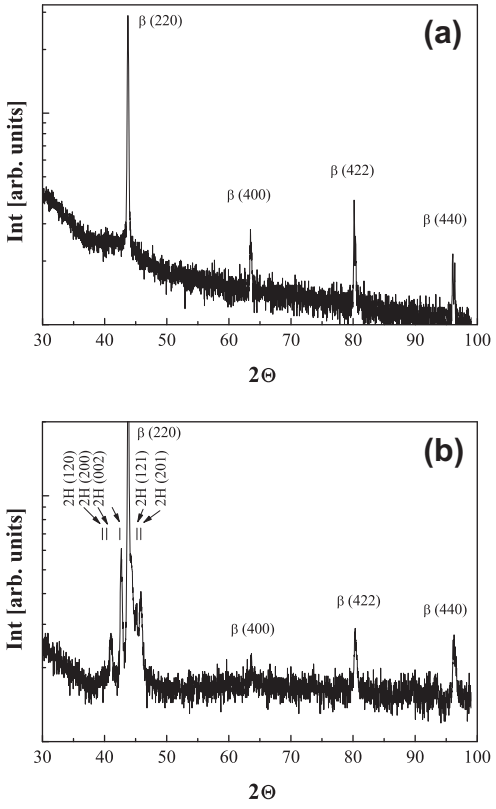

Fig. 2. (a) X-ray diffraction pattern at room temperature in a Cu–Zn–Al (F1) film obtained by reactive thermal annealing. The peaks were indexed according to the $L2_1$ structure. (b) X-ray diffraction pattern at room temperature in a Cu–Zn–Al (F2) film obtained by reactive thermal annealing. The peaks were indexed according to the $L2_1$ structure and to the 2H martensitic structure.

were indexed according to the cubic $L2_1$ structure. Even though superlattice faint reflections corresponding to 200 and 111 type cannot be observed, their presence is confirmed by the TEM results described below. In film F2 the martensitic transformation starts at 290 K (Table 1) and, therefore, coexistence between β and 2H martensite can be observed at room temperature. Fig. 2b shows an X-ray diffraction pattern of film F2 at room temperature were β and 2H martensite peaks can be observed [28].

TEM results in film F1 are shown in Fig. 3. The microstructure of the β phase and an electron diffraction pattern corresponding to one grain oriented along the $[110]_{L21}$ zone axis are shown in Fig. 3(a and b), respectively. From this orientation, superlattice 002 and 111 type reflections can be observed, together with additional reflections corresponding to surface martensite (SM) [29]. This surface martensite can be attributed to either poor zinc or poor aluminum surface composition as a consequence of different ion etching during the TEM sample preparation. TEM results in film

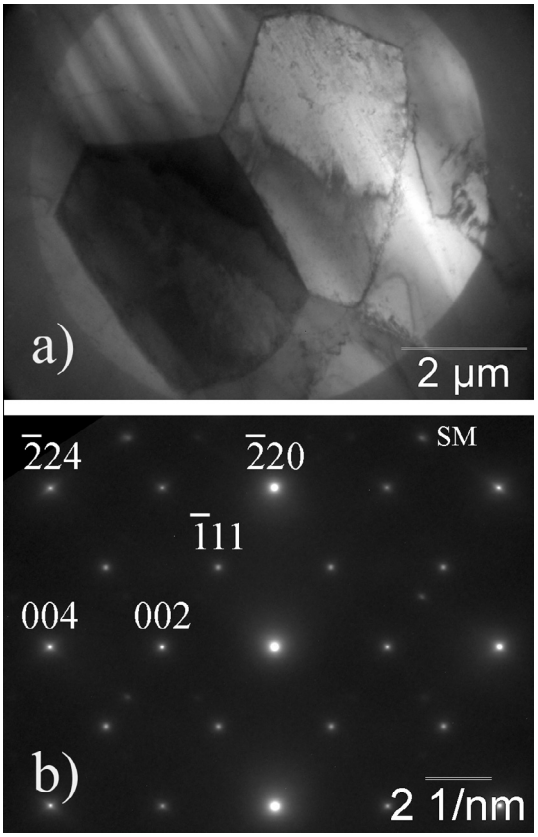

Fig. 3. TEM results in film F1. (a) Bright field image of the microstructure. (b) [110] electron diffraction pattern of the $L2_1$ structure corresponding to the β phase. SM refers to surface martensite reflection.

F2 can be observed in Fig. 4. The microstructure of the film in austenite at room temperature is shown in Fig. 4(a and b) shows the [001] electron diffraction pattern of the $L2_1$ structure of the austenite with additional reflections corresponding to a γ-phase precipitate [30]. These precipitates have a typical size of about 100 nm and they affect the M_s value and features associated with the martensitic transformation, such as hysteresis and mechanical response. The precipitation of γ-phase could have been originated during the heating to 1123 K as the film precursor P2 has a higher Al content, and passes through a γ and β two-phase stability field. Such precipitates eventually would not dissolve during the annealing in the β stability region. Initially, it would be possible to avoid the presence of precipitates, either by annealing for longer periods of time or by increasing the annealing temperature [30]. However, degradation of the thin film due to evaporation/oxidation will occur. Nevertheless, as it has been discussed in Ref. [27], the presence of precipitates may have interesting effects on the martensitic transformation. Fig. 4(c and d) correspond to film F2 in martensite and show a TEM image of the microstructure and an electron diffraction pattern of the twinned 2H martensite along the $[2\bar{1}0]_{2H}$ orientation, respectively. To ensure the presence of martensite at RT, as expected from electrical transport data presented in Fig. 1, film F2 was cooled down to liquid nitrogen before thinning for TEM. Average grain size was measured from several TEM images and different results were obtained in each sample, being (3 ± 1) μm in film F1 and (1.3 ± 0.9) μm in film F2. An inhomogeneous distribution of the grain size between films was shown. This is probably related to the film growth process.

The results presented here and in previous studies in Cu–Zn [31]and Cu–Zn–Al [21] films show that the features of the transformation depend on both the type of martensitic structure and on

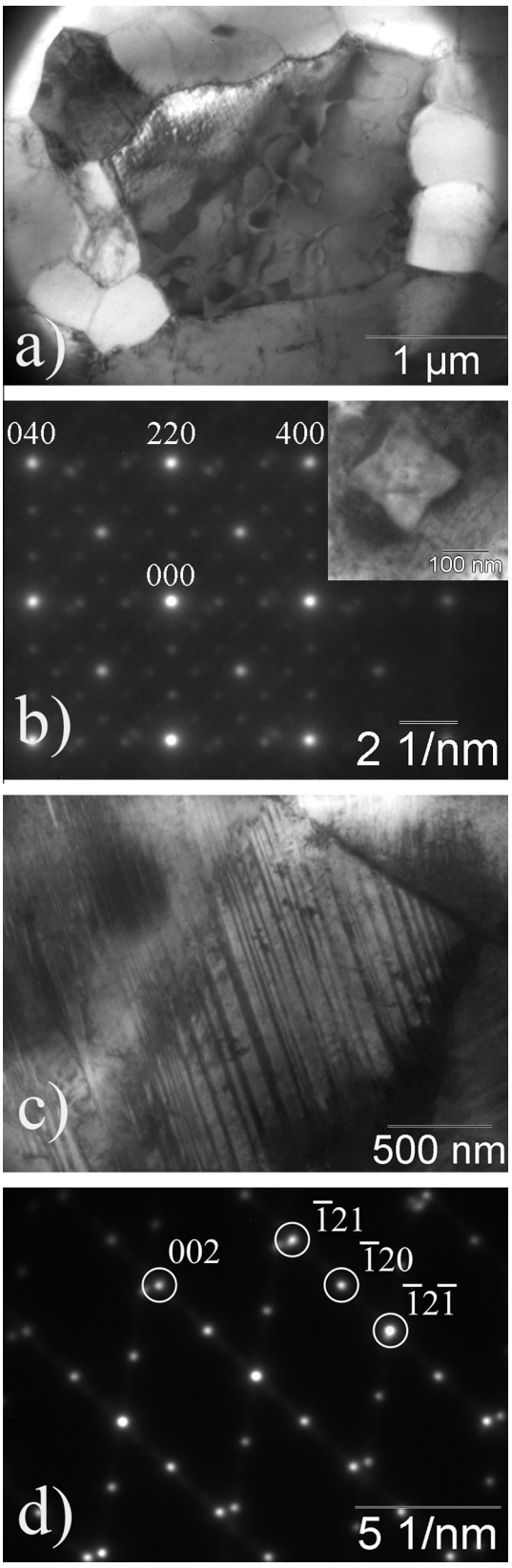

Fig. 4. Film F2. (a) After heating, the film is mainly in the β phase with the $L2_1$ structure. Antiphase boundaries can be observed in some grains. (b) [1 0 0] Electron diffraction pattern of the β phase with additional reflections corresponding to a γ-phase precipitate (inset). (c) After cooling, the film is in 2H martensite. Twinned variants can be observed. (d) Electron diffraction pattern of the twinned 2H martensite from a $[2\,1\,0]_{2H}$ orientation.

the microstructure of the films. Cu–Zn–Al films with β → 18R transformation and with average grain size ≈1 μm present a higher hysteresis (35–50 K) compared to bulk samples (≈5 K) [21], whereas films with β → 2H transformation and similar microstructure present hysteresis similar to those found in bulk reference samples.

The differences in the hysteresis of the transformation induced by temperature in different bulk martensitic systems have been discussed by Ahlers in Ref. [32]. The martensitic transformation can be decomposed into three steps: the nucleation, the lateral expansion of thin martensite plates at constant thickness, and their thickening. The nucleation usually occurs at crystalline defects such as dislocations [33]. The habit plane is propagated by minimizing the elastic deformation around the tip. Once a thin martensite plate is created, it often thickens by the movement of the interfaces. The large hysteresis in Cu–Zn–Al films with β → 18R martensitic transformation should be understood by considering the influence of the microstructure in the progression of the transformation, which induces internal stresses and reduces the local temperature of coexistence among the two phases. A considerable overcooling or overheating around $T_0 = (A_f - M_s)/2$, which is manifested as a large hysteresis, should be induced in order to produce the transformation and retransformation in comparison with bulk samples with larger grain size. The stress field produced by small grains in the transformation path is evident considering the high mechanical performance of sub micrometric free Cu–Ni–Al nanopilars [10]. The smaller influence of micrometric grains in the β → 2H transformation of Cu–Zn–Al films is related with the intrinsic features of temperature-driven martensitic phase transformation. The mechanism of formation of 2H martensite is different than those found in 9R or 18R martensite [32]. The transformation starts with the formation of a nucleus of the untwinned 2H martensite, which creates stresses in the surrounding matrix. These stresses can only be released when the necessary driving force is available to relax the stresses (after cooling) by activating a twin shear in the already formed 2H martensite. In this case, the overcooling required to produce the nucleation of the 2H martensitic structure reduces the influence of the microstructure on the temperature driven transformation, in comparison to the one found in films with 18R martensite transformation.

Another feature associated with the β → 2H transformation is the absence or difficulty to obtain the double-shape-memory effect, which is related with the capacity to memorize two different geometries in the austenitic and martensitic phases after undergoing a specific thermo mechanical treatment (“training treatment”). Although films with β → 18R transformation present large hysteresis, it is possible to train them by inducing the same deformation in different thermal cycles [21]. However, the same type of training is hard to perform in films with the β → 2H transformation, despite the similarity in the transformation path with bulk samples. This fact has been discussed in Ref. [34] by considering the nucleation difficulties in bulk SMA with large hysteresis. It is important to mention that double shape memory effect in samples with 2H structure can be improved by the inclusion of nano precipitates [27]. The modification of the microstructure could enhance the performance of these films for technological applications based on tunable martensitic transformation and double-shape-memory effect.

4. Conclusions

In summary, it has been demonstrated that it is possible to produce SMA Cu–Zn–Al films with β → 2H martensitic transformation by fixing $e/a \approx 1.53$. The transformation temperature and the hysteresis associated to the transformation in the films are close

to those found in bulk samples. This study shows that these features (in $\beta \rightarrow 2H$ transformation) are less sensitive to the microstructure compared to the $\beta \rightarrow 18R$ transformation. This fact has been associated with the intrinsic nature of the transformation that needs substantial undercooling to produce the nucleation of the martensitic phase. The necessary driving force for the burst-type martensitic transformation is not sensitive to the stress field produced by small grains.

Acknowledgments

We thank to C. Gómez Bastidas, C. Cotaro, I. Artola, E. Aburto and M. Isla for technical assistance. This work has been supported by Agencia Nacional de Promoción Científica y Tecnológica, PICT 07-02284, UN Cuyo – 2011- 06/C355, and CONICET PIP 2010-0457. N. H and J. G. are members of the Instituto de Nanociencia y Nanotecnología (Argentina). N.H., A.M.C. and J.G. are members of CONICET (Argentina).

References

[1] K. Otsuka, X. Ren, Prog. Mater. Sci. 50 (2005) 511–678.
[2] Y. Fu, H. Du, W. Huang, S. Zhang, M. Hu, Sens. Actuators, A: Phys. 112 (2004) 395–408.
[3] Stephen.A. Wilson et al., Mater. Sci. Eng. R 56 (2007) 1–129.
[4] Tobias. Edler, Stefan.G. Mayr, Adv. Mater. 2 (2010) 4969–4972.
[5] N. Ozdemir, I. Karaman, N.A. Mara, Y.I. Chumlyakov, H.E. Karaca, Acta Mater. 60 (2012) 5670–5685.
[6] Artemy Irzhak, Viktor Koledov, Dmitry Zakharov, Gor Lebedev, Alexey Mashirov, Veronika. Afonina, Kristina Akatyeva, Vladimir. Kalashnikov, Nikolay Sitnikov, Natalia. Tabachkova, Alexander Shelyakov, Vladimir Shavrov, J. Alloys Comp. 586 (2014) 5464–5468.
[7] D.D. Shin, K.R. Mohanchandra, G.P. Carman, Sens. Actuators, A – Phys. 119 (2005) 151–156.
[8] S.C. Mao, H.X. Li, Y. Liu, Q.S. Deng, L.H. Wang, Y.F. Zhang, Z. Zhang, X.D. Han, J. Alloys Comp. 579 (2013) 100–111.
[9] Yuan. Zhong, Ken. Gall, Ting. Zhu, Acta Mater. 60 (2012) 6301–6311.
[10] M. Jose, San Juan, L.Nó. Maria, Christopher A. Schuh, Adv. Mater. 20 (2008) 272–273.
[11] J. San Juan, M.L. Nó, C.A. Schuh, Acta Mater. 60 (2012) 4093–4106.
[12] C.P. Frick, S. Orso, E. Arzt, Acta Mater. 55 (2007) 3845–3855.
[13] M. Ahlers, Prog. Mater. Sci. 30 (1986) 135–186.
[14] M. Ahlers, J.L. Pelegrina, Acta Metall. Mater. 40 (1992) 3213–3220.
[15] J.L. Pelegrina, M. Ahlers, Acta Metall. Mater. 38 (1990) 293–299.
[16] J.L. Pelegrina, M. Ahlers, Acta Metall. Mater. 40 (1992) 3221–3227.
[17] S. Miyazaki, A. Ishida, Mater. Sci. Eng. A 273–275 (1999) 106–133.
[18] S. Miyazaki, T. Hashinaga, A. Ishida, Thin Solid Films 281–282 (1996) 364–367.
[19] W. Huang, Mater. Des. 23 (2002) 11–19.
[20] Lei. Qiao, Raul. Radovitzky, Acta Mater. 61 (2013) 6213–6221.
[21] N. Haberkorn, F.C. Lovey, A.M. Condó, J. Guimpel, Mater. Sci. Eng. B 170 (2010) 5–8.
[22] T. Waitz, D. Spisâk, J. Hafner, H.P. Karnthaler, Europhys. Lett. 71 (2005) 98–102.
[23] T. Waitz, T. Antretter, F.D. Fischer, N.K. Simha, H.P. Karnthaler, J. Mech. Phys. Solids 55 (2007) 419–444.
[24] M. Sade, private communication.
[25] J. L. Pelegrina, private communication.
[26] G. Petzow, G. Effenberg, Ternary Alloys, vol. 4, VCH Verlagsgesellschaft mbH, Weinheim, 1988.
[27] F.C. Lovey, V. Torra, Prog. Mater. Sci. 44 (1999) 189–289.
[28] F. Saule, M. Ahlers, F. Kropff, E. B. Rivero, Acta Metall. Mater. 40 (1992) 3229–3238.
[29] F.C. Lovey, M. Chandrasekaran, Acta Metall. 31 (1983) 1919–1927.
[30] F.C. Lovey, G. Van Tendeloo, J. Van Landuyt, M. Chandrasekaran, S. Amelinckx, Acta Metall. 32 (1984) 879–886.
[31] N. Haberkorn, M. Ahlers, F.C. Lovey, Script. Mater. 61 (2009) 821–824.
[32] M. Ahlers, Phil. Mag. A 8 (2002) 1093–1114.
[33] A. Ibarra, D. Caillard, J. San, Juan, M. L. Nó, Appl. Phys. Lett. 90 (2007) 101907–101910.
[34] L. Delaey, H. Warlimont, Shape Memory Effects in Alloys (1975) 89–144.